Sensors & Actuators: B. Chemical 450 (2026) 139265

Contents lists available at ScienceDirect

Sensors and Actuators: B. Chemical

journal homepage: www.elsevier.com/locate/snb

Detecting $^{14}CO_2$ with two-photon absorption spectroscopy

Y.-D. Tan [a,*], Y.-Z. Liu [b], M.-Y. Yu [a], Z.-N. Wang [a], C.-F. Cheng [a,c], S.-M. Hu [a,c,d]

[a] Hefei National Research Center for Physical Sciences at the Microscale, University of Science and Technology of China, Hefei, 230026, China
[b] School of Physical Sciences, University of Science and Technology of China, Hefei, 230026, China
[c] Hefei National Laboratory, University of Science and Technology of China, Hefei, 230088, China
[d] State Key Laboratory of Chemical Reaction Dynamics, University of Science and Technology of China, Hefei, 230026, China

ARTICLE INFO

Keywords:
Optical gas sensor
Radiocarbon
Laser spectroscopy

ABSTRACT

We present an optical detection method for $^{14}CO_2$ using mid-infrared two-photon absorption (TPA) spectroscopy. Leveraging a custom-built optical parametric oscillator (OPO) and a high-finesse cavity, we demonstrate sub-parts-per-billion (ppb) detection limits for $^{14}CO_2$ at room temperature. The technique exploits the Q(14) vibrational transition at 4516 nm, where near-resonant intermediate states enhance TPA signals while suppressing interference from abundant isotopologues such as $^{13}CO_2$. Cavity-enhanced detection, combined with active frequency stabilization, enables precise measurements with a detection limit of 0.4 ppb. Theoretical analysis confirms the method's potential to reach the natural abundance level (0.0012 ppb) with higher laser power, addressing critical challenges in monitoring nuclear facility emissions and fossil-fuel-derived CO_2. The results pave the way for field-deployable systems for real-time, in situ monitoring of atmospheric $^{14}CO_2$.

1. Introduction

Carbon-14 is the only long-lived radioactive carbon isotope. It is produced at a nearly constant rate in the atmosphere through the $^{14}N(n,p)^{14}C$ reaction, where thermal neutrons generated by cosmic rays or nuclear waste interact with atmospheric nitrogen [1]. Once formed, ^{14}C rapidly oxidizes and exists primarily as carbon dioxide. With a half-life of 5700 years, beta decay results in a natural $^{14}C/C$ abundance of approximately 1.2 parts per trillion (ppt) [2,3]. Despite its low concentration, this stability makes ^{14}C highly useful in applications such as radiocarbon dating. Additionally, ^{14}C serves as a critical tracer for distinguishing fossil fuel-derived CO_2 (ff-CO_2) from biogenic or atmospheric CO_2 fluxes [4,5]. Since fossil fuels have undergone complete radioactive decay over geological timescales, ff-CO_2 contains no detectable ^{14}C. Conversely, elevated ^{14}C levels are found in nuclear waste, including reactor components [6,7], ion exchange resins, and moderator graphite [8]. Consequently, measuring $^{14}CO_2$ concentrations is essential for monitoring potential leaks from nuclear facilities. Given CO_2's rapid atmospheric diffusion, accurate quantification of $^{14}CO_2$ near such sites is vital for radiation protection and environmental safety.

Conventional techniques for detecting $^{14}CO_2$, such as accelerator mass spectrometry (AMS) and liquid scintillation counting (LSC), are laboratory-based and require extensive sample preparation, making real-time, in situ monitoring impractical [9–12]. Given the importance of monitoring $^{14}CO_2$ around nuclear facilities, developing online measurement methods is essential. Optical detection techniques, with their non-invasive nature, rapid response, and in situ capabilities, offer a promising solution and have garnered significant international interest. Over the past two decades, cavity-enhanced spectroscopy has emerged as a powerful tool for detecting $^{14}CO_2$ [13–18]. For enriched samples (~ 10 ppb), spectral interference is less problematic, enabling robust measurements. A Finnish group has further validated this approach for tracing nuclear facility emissions [14,17]. Due to the extremely low natural abundance of ^{14}C, optical detection based on single-photon absorption (SPA) faces major challenges, including spectral interference from abundant isotopologues (e.g., $^{13}CO_2$) and other atmospheric absorbers. The absorption interference from CO_2 isotopologues mainly originates from their hot-band transitions, which diminish at lower temperatures. Galli et al. pioneered the use of cryogenic SPA spectroscopy, achieving detection sensitivities as low as 5 ~ 10 parts-per-quadrillion (ppq) [19,20]. However, these methods require stringent experimental conditions, primarily due to the use of cryogenic cooling systems. To overcome limitations in resolution in

* Corresponding author.
E-mail addresses: tyd2018@mail.ustc.edu.cn (Y.-D. Tan), cfcheng@ustc.edu.cn (C.-F. Cheng), smhu@ustc.edu.cn (S.-M. Hu).

https://doi.org/10.1016/j.snb.2025.139265
Received 28 July 2025; Received in revised form 11 November 2025; Accepted 1 December 2025
Available online 2 December 2025

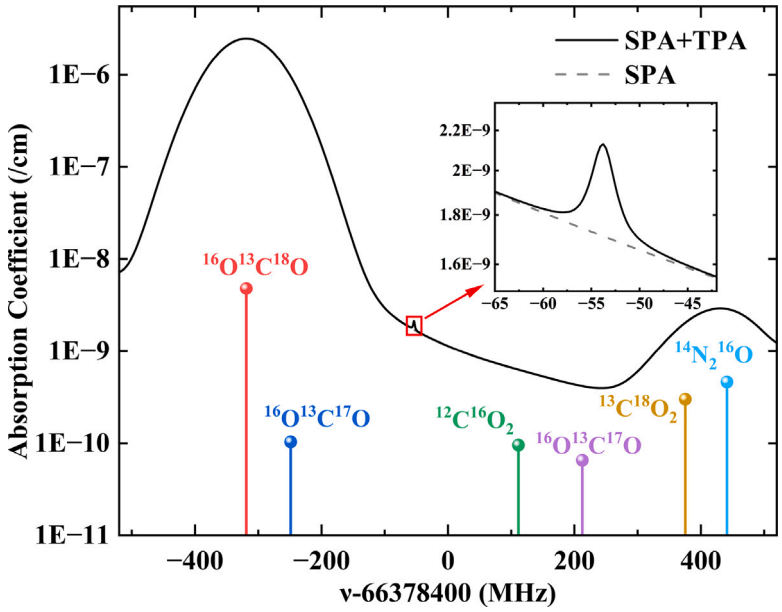

Fig. 1. Simulated single-photon absorption (SPA) and two-photon absorption (TPA) spectra near 4516 nm. The inset shows the two-photon absorption peak of $^{14}CO_2$ at a concentration of 70 ppb. Vertical lines in different colors indicate the absorption lines of other isotopologues/molecules in the sample. Note that the $^{14}N_2{}^{16}O$ line also contributes to the SPA signal. In the simulation, nitrous oxide concentration was set to 1 ppb in the CO_2 sample with a total pressure of 50 Pa at 296 K.

principle, a double-resonance spectroscopic technique utilizing two-wavelength lasers has been proposed [21], significantly improving spectral discrimination. Although molecular energy transfer processes make double-resonance spectroscopy measurements sensitive to drifts in laser power and sample pressure, the method has great potential in trace detection. Jiang et al. have, for the first time, experimentally demonstrated room-temperature detection of radiocarbon dioxide ($^{14}CO_2$) molecules in ~ 1.5× natural abundance CO_2 samples, achieving a sensitivity of 1.4 parts-per-quadrillion (ppq, 10^{-15}) in terms of average measurement precision and a quantitation accuracy of 4.6 ppq [22,23].

An alternative approach — one-color two-photon absorption (TPA) using a single laser — was initially proposed by Lehmann et al. [24,25] and has recently been experimentally demonstrated by our group [26,27]. These experiments confirmed the quantitative detection capability of two-photon spectroscopy: measurements of $^{13}CO_2$ samples at varying concentrations, cross-validated with isotope ratio mass spectrometry (IRMS), achieved a detection accuracy of 0.5%, meeting the requirements for high-precision carbon isotope analysis. This high-resolution, narrow-linewidth approach is therefore highly suitable for $^{14}CO_2$ detection. As shown in Fig. 1, the simulated TPA spectrum is clearly distinguishable from conventional SPA spectra arising from major CO_2 isotopologues and other molecules, such as N_2O. It should also be noted that dominant atmospheric components, such as N_2, O_2, and Ar, contribute to neither SPA nor TPA spectra in the spectral region of interest. Most water vapor can be effectively removed from air samples using a cold trap at approximately −70 °C without considerable loss of CO_2, and residual trace H_2O does not introduce absorption features near 4.5 μm. Therefore, the TPA method offers a feasible route for detecting $^{14}CO_2$ in atmospheric samples. Nevertheless, the development of practical $^{14}CO_2$ optical sensors based on TPA has so far been hindered by the limited availability of high-power laser sources in the relevant mid-infrared region.

In this work, we report the first implementation of a two-photon spectroscopic sensor for detecting $^{14}CO_2$, enabled by a custom-built mid-infrared OPO light source. The system achieves a sub-parts-per-billion (ppb) detection limit, with clear spectral discrimination demonstrated for $^{14}CO_2$ concentrations of 71 ppb and 2 ppb. Supported by theoretical analysis, our results confirm the feasibility of extending this approach to natural-abundance samples, highlighting its promise for high-precision environmental monitoring.

2. Experiment

The experimental setup is schematically presented in Fig. 2. Mid-infrared light from a home-made continuous-wave OPO source [28,29] is coupled into a high-finesse cavity. The cavity comprises two low-loss mirrors with a reflectivity of $R \approx 99.995\%$ in the range from 4500 to 4550 nm. The mirrors have radii of curvature of 1 m and are spaced 40 cm apart, yielding a Gaussian beam waist of about 0.76 mm at the focus. The measured ring-down time of the empty cavity is about 30 μs and the circulating intra-cavity laser power is enhanced by a factor of 5082 relative to the input power, as calculated according to Ref. [30].

In two-photon absorption spectroscopy measurements, the OPO mid-infrared idler light is locked to the high-finesse cavity. The OPO's pump light, with a linewidth of 10 kHz (integrated over 100 μs), is locked to an ultra-low expansion glass (ULE) cavity using the Pound-Drever-Hall (PDH) method. A second PDH loop locks the OPO idler light to the high-finesse cavity, with the fast feedback signal sent to the electro-optical modulator (EOM) placed inside the OPO cavity and the slow feedback signal sent to a piezo actuator attached to one of the OPO cavity mirrors. Therefore, the frequency drift of the longitudinal mode of the high-finesse cavity is transferred to that of the OPO mid-infrared idler light, which can be monitored by measuring the OPO's signal light frequency since the OPO's pump light frequency has been locked. To further stabilize the cavity length and the idler frequency, a frequency reference is employed, such as near-infrared optical frequency comb (OFC) referenced to a GPS-disciplined clock (accuracy 1.2×10^{-12}). The OFC records the frequencies of the OPO's pump and signal beams by measuring the offsets (Δf_p and Δf_s) between these beams and their nearest comb lines. The difference ($\Delta f_p - \Delta f_s$) is used in a phase

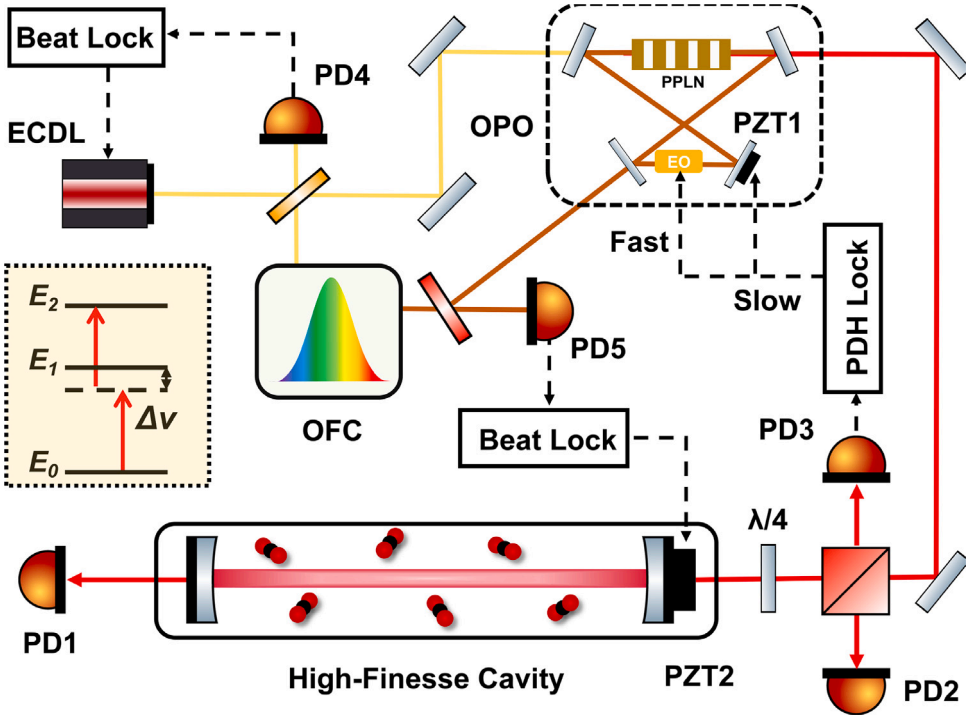

Fig. 2. Schematic diagram of mid-infrared cavity-enhanced two-photon device and molecular transition energy level diagram. Abbreviations: ECDL, external cavity diode laser; PD, photodetector; OPO, optical parametric oscillator; PPLN, periodically poled lithium niobate; EO, electro-optic modulator; PZT, piezoelectric transducer; OFC, optical frequency comb.

lock loop (PLL) to generate a feedback signal, which is applied to a piezoelectric actuator attached to one of the cavity mirrors. This active stabilization suppresses cavity length fluctuations [31,32]. For precise MIR frequency scans, the PLL's reference microwave function generator is finely adjusted. The transmitted cavity power is detected using a HgCdTe amplified photodetector (PD1), while a second photodetector (PD2) monitors the input power to account for long-term fluctuations.

We define the dimensionless amplitude of the TPA signal, S_{TPA}, using the cavity transmittance κ at the center frequency ν_0:

$$\kappa \equiv \frac{P_{ic}(\nu_0)}{P_{ic,0}}, \tag{1}$$

$$S_{TPA} \equiv \frac{1-\kappa}{\kappa^2} = \frac{\gamma_2 P_{ic,0}}{\gamma_0}, \tag{2}$$

where P_{ic} and $P_{ic,0}$ are intra-cavity laser powers with and without the two-photon absorption, respectively; γ_2 is the two-photon absorption rate proportional to the mole fraction of the analyte [24], $\gamma_0 = c(1-R)/L$ is the cavity loss rate without absorption from the sample, c is the speed of light, R is the reflectivity of the cavity mirror, and L is the distance between two cavity mirrors. The TPA signal can be enhanced by either (1) using mirrors with higher reflectivity and lower loss [33,34], which reduces γ_0, or (2) increasing the input laser power (before signal saturation occurs), thereby boosting $P_{ic,0}$. The detailed derivations of the formulas can be found in our previous work [26].

3. Result and discussion

To measure the TPA signal of $^{14}CO_2$, we utilize the vibrational transition with the largest two-photon absorption coefficient (γ_2). Specifically, we select Q(14) transition from the $J = 14$ (00001) state to the $J = 14$ (00021) state at 4516 nm, chosen for two key reasons: (i) The asymmetric stretching fundamental band provides the strongest vibrational transition in the molecule. (ii) The near-resonant transition group, P(14) (00001 → 00011) and R(13) (00011 → 00021), has the closest frequency detuning, minimizing the laser resonance mismatch and significantly enhancing the two-photon transition rate [22,35–37]. While two-photon transitions are ubiquitous in molecules, most are challenging to observe due to weak transition dipole moments and large detuning from near-resonant states.

As a demonstration, we measured two carbon dioxide gas samples with $^{14}CO_2$ abundances of 71 ± 11 ppb and 2 ± 0.3 ppb. The 71 ppb sample was measured at a gas pressure of 47 Pa and a circulating laser power of approximately 20 W, with the raw spectrum shown in Fig. 3(a). The Doppler-free nature of TPA results in a linewidth that is significantly narrower than that of adjacent SPA features, exceeding two orders of magnitude in reduction compared to SPA transitions, thereby greatly enhancing spectral selectivity. As shown in Fig. 3(b), the SPA contribution manifested as a linear background that was removed during transmittance signal normalization [26]. Using Eq. (2), we derived the TPA signal amplitude of 2.5×10^{-3} with a linewidth of 2.01 ± 0.04 MHz, as shown in Fig. 3(c). This amplitude is consistent with the calculated value of 4.5×10^{-3}, supporting the validity of the computational model. For our analysis, Voigt profile fitting served as a reasonable approximation, while more rigorous solutions to the line profile model can be found in Refs. [24,38,39], and Eq. (2) provides an exact solution only at exact resonance conditions. It should be noted that theoretical calculations are used to guide predictions of two-photon signal strength and the selection of experimental conditions, and the sample concentration is obtained via calibration against standard samples, as detailed in our previous work [26].

According to Eq. (2), at a fixed sample concentration, the TPA signal amplitude increases proportionally with intra-cavity laser power and gas pressure before saturation [26]. In contrast, for SPA, the saturation parameter increases with power, resulting in signal reduction [40]. Furthermore, the saturation power for TPA is inherently higher than

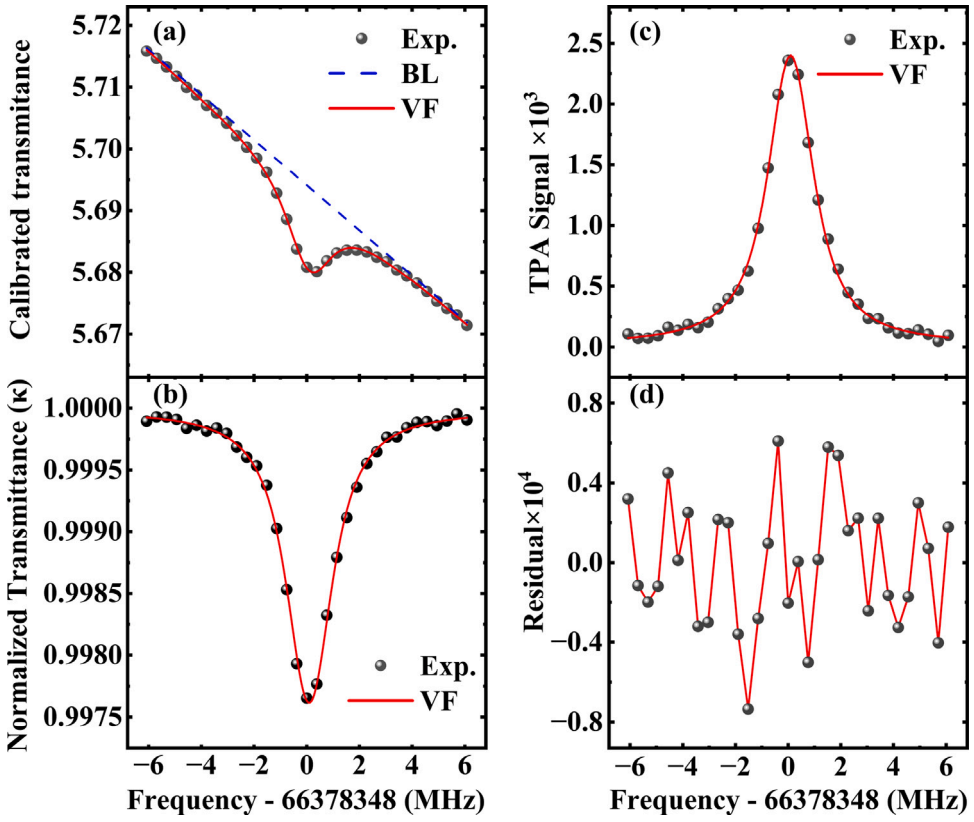

Fig. 3. The two-photon spectral diagrams of $^{14}CO_2$ at a concentration of 71 ppb obtained under 20 W power and 47 Pa pressure conditions, where (a) is the spectrogram directly obtained from the experiment, (b) is the normalized transmittance spectrogram obtained after baseline subtraction, and (c) is its corresponding two-photon absorption spectrogram. (d) The residuals obtained from the Voigt fitting in (c). Abbreviations: Exp: Experimental; BL: Baseline; VF: Voigt fitting.

that for SPA. Consequently, under identical concentration and pressure conditions, increasing the laser power enhances the TPA signal while simultaneously suppressing the SPA signal. This observed power-dependent behavior unambiguously confirms the anticipated trade-off between TPA enhancement and SPA suppression. Fig. 4 shows the averaged result of 1264 spectra of a 2 ppb $^{14}CO_2/CO_2$ sample, with each spectrum acquired over approximately 50 s. To compensate for the low concentration, the sample pressure and intra-cavity power were increased to 299 Pa and 83 W, respectively. The resulting spectrum exhibits a broadened linewidth of 13.4 ± 1.7 MHz and yields a noise-equivalent detection limit of about 0.4 ppb ($k = 3$).

The system's ultimate sensitivity remains fundamentally limited by available intra-cavity laser power. This two-photon absorption technique exhibits particular advantages for atmospheric monitoring applications due to its narrow linewidth and immunity to interference from nearby absorbers, making the method ideally suited for challenging detection scenarios such as radiocarbon emission monitoring in nuclear facilities [17].

To evaluate the potential of the TPA approach, we calculated the $^{14}CO_2$ abundance ($^{14}C/C$) that can be detected under current noise-equivalent detection limit (TPA signal about 1×10^{-5}), using spectral parameters from Ref. [37] at 4516 nm under varying pressures and laser powers, based on the current experimental setup. The calculations employed an approximate analytical formula, valid under the condition that the laser-induced Rabi frequency remained significantly smaller than the detuning ($\Delta\nu$) [24,26]. When the Rabi frequency becomes comparable to the detuning, the approximate $^{14}C/C$ underestimates the numerical solution of the density matrix by less than 50%. Nevertheless, this level of accuracy suffices to demonstrate the prospective signal trends. Previous quantitative measurements of $^{14}C/C$ ratios were conducted under low sample pressures and laser powers (red triangle and square in Fig. 5). On the contour plot, the yellow dot-dashed lines mark the experimental conditions where the TPA linewidth corresponds to 1% and 10% of the single-photon absorption (SPA) linewidth. A narrower TPA linewidth indicates enhanced selectivity, highlighting the method's potential for highly discriminative detection.

We have confirmed [26] a clear scaling relationship between the TPA signal and both laser power and gas pressure, and demonstrated [41] the attainment of an intra-cavity infrared laser power up to 2 kW. This combination of a validated scaling law and high achievable power establishes a clear pathway toward significantly enhanced sensitivity and, ultimately, detection at natural abundance. Future advances in high-power lasers, cavity mirror coatings, and noise suppression techniques — such as active noise-eater stabilization or frequency modulation spectroscopy — will further solidify the promise of this TPA-based approach for measuring naturally abundant $^{14}CO_2$. A key advantage of our sensor lies in its ability to perform cavity-enhanced detection using a single laser source operating at room temperature, significantly reducing instrumental complexity. This feature is particularly advantageous for scalable, in situ atmospheric monitoring deployments. Furthermore, the methodology is readily adaptable to the detection of other trace molecular species or radicals. In particular, polyatomic molecules offer dense rovibrational transition spectra, which provide a wealth of near-resonant intermediate states and thereby facilitate efficient enhancement of TPA signals.

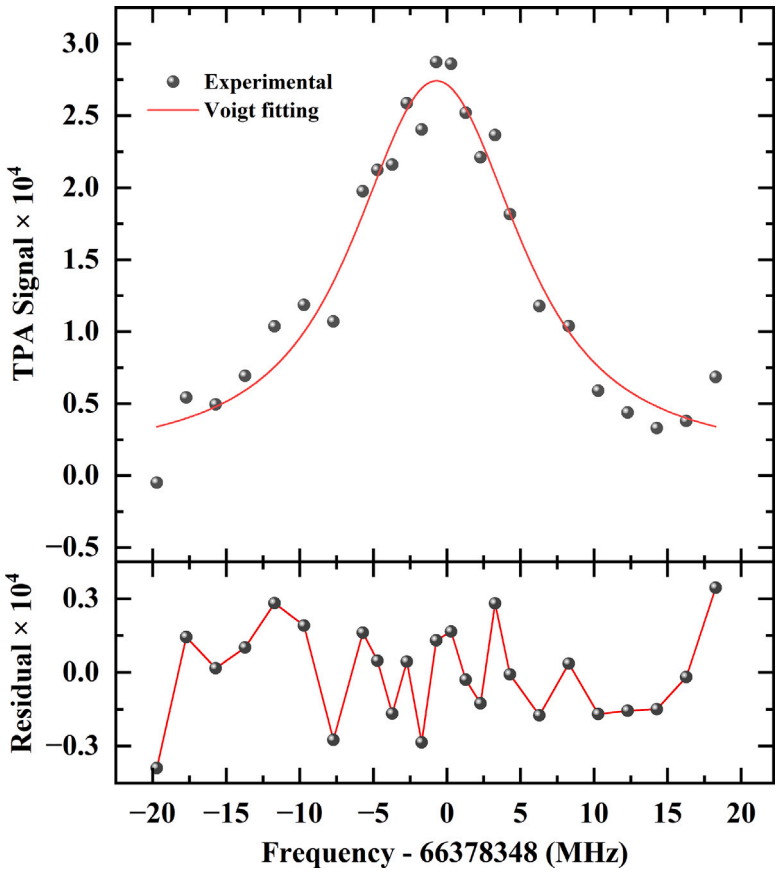

Fig. 4. The two-photon spectrum of $^{14}CO_2$ at a concentration of 2 ppb obtained under a circulating laser power of 83 W and sample pressure of 299 Pa. The upper panel shows the normalized TPA spectrum, and the lower panel gives the corresponding fitting residuals.

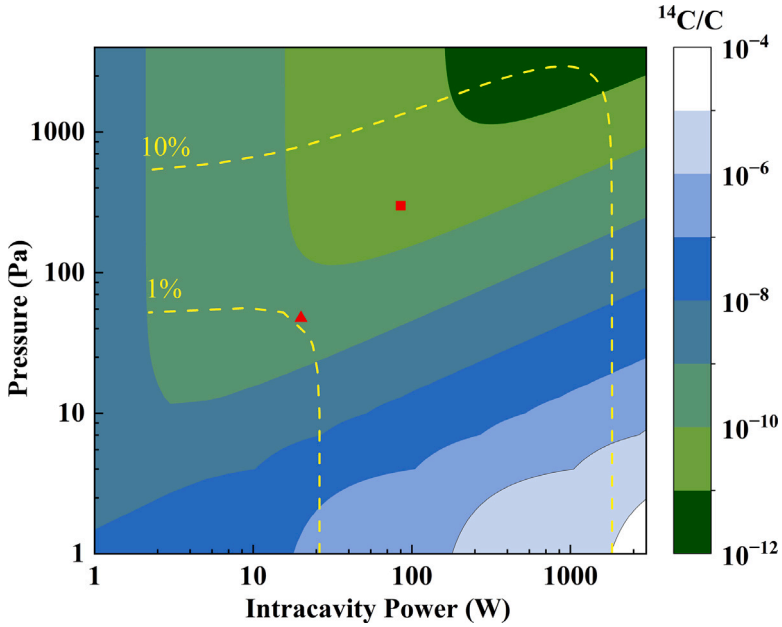

Fig. 5. Minimum detectable concentrations of $^{14}CO_2$ under different pressure and power conditions at a two-photon absorption (TPA) detection limit of 1×10^{-5}. Two yellow dash-dot lines indicate experimental conditions where TPA linewidths are 1% and 10% of the single-photon absorption (SPA) linewidth. Red triangles and squares represent the pressure and laser power conditions used for the TPA spectra of $^{14}CO_2$ at concentrations of 71 ppb (Fig. 3) and 2 ppb (Fig. 4), respectively.

CRediT authorship contribution statement

Y.-D. Tan: Writing – review & editing, Writing – original draft, Visualization, Validation, Data curation, Conceptualization. **Y.-Z. Liu:** Data curation. **M.-Y. Yu:** Formal analysis, Data curation. **Z.-N. Wang:** Data curation. **C.-F. Cheng:** Writing – review & editing, Writing – original draft, Supervision, Project administration, Funding acquisition, Conceptualization. **S.-M. Hu:** Supervision, Project administration, Methodology, Funding acquisition, Conceptualization.

Declaration of competing interest

The authors declare that they have no known competing financial interests or personal relationships that could have appeared to influence the work reported in this paper.

Acknowledgments

This work was jointly supported by the Innovation Program for Quantum Science and Technology (Grant Nos. 2021ZD0303102, 2023ZD0301000), the Chinese Academy of Sciences (Grant Nos. YSBR-055, XDB0970100), and the National Natural Science Foundation of China (Grant Nos. 22241302, 12393825).

Data availability

Data will be made available on request.

References

[1] R.E. Lingenfelter, Production of carbon 14 by cosmic-ray neutrons, Rev. Geophys. 1 (1) (1963) 35–55.
[2] H. Godwin, Half-life of radiocarbon, Nature 195 (4845) (1962) 984–984.
[3] W. Kutschera, The half-life of ^{14}C – why is it so long? Radiocarbon 61 (5) (2019) 1135–1142.
[4] J. Turnbull, P. Rayner, J. Miller, T. Naegler, P. Ciais, A. Cozic, On the use of $^{14}CO_2$ as a tracer for fossil fuel CO_2: Quantifying uncertainties using an atmospheric transport model, J. Geophys. Res. 114 (D22) (2009) 984–984.
[5] H.E. Suess, Radiocarbon concentration in modern wood, Science 122 (3166) (1955) 415–417.
[6] G. Zazzeri, E.A. Yeomans, H. Graven, Global and regional emissions of radiocarbon from nuclear power plants from 1972 to 2016, Radiocarbon 60 (4) (2018) 1067–1081.
[7] M.-S. Yim, F. Caron, Life cycle and management of carbon-14 from nuclear power generation, Prog. Nucl. Energy 48 (1) (2006) 2–36.
[8] L. Payne, P.J. Heard, T.B. Scott, Examination of surface deposits on oldbury reactor core graphite to determine the concentration and distribution of ^{14}C, PLoS One 11 (10) (2016) e0164159.
[9] C.L. Bennett, R.P. Beukens, M.R. Clover, H.E. Gove, R.B. Liebert, A. Litherland, K.H. Purser, W.E. Sondheim, Radiocarbon dating using electrostatic accelerators: negative ions provide the key, Science 198 (4316) (1977) 508–510.
[10] D.E. Nelson, R.G. Korteling, W.R. Stott, Carbon-14: direct detection at natural concentrations, Science 198 (4316) (1977) 507–508.
[11] H. Woo, S. Chun, S. Cho, Y. Kim, D. Kang, E. Kim, Optimization of liquid scintillation counting techniques for the determination of carbon-14 in environmental samples, J. Radioanal. Nucl. Chem. 239 (1999) 649–655.
[12] X. Hou, Liquid scintillation counting for determination of radionuclides in environmental and nuclear application, J. Radioanal. Nucl. Chem. 318 (3) (2018) 1597–1628.
[13] D. Labrie, J. Reid, Radiocarbon dating by infrared laser spectroscopy: A feasibility study, Appl. Phys. A 24 (4) (1981) 381–386.
[14] G. Genoud, J. Lehmuskoski, S. Bell, V. Palonen, M. Oinonen, M.-L. Koskinen-Soivi, M. Reinikainen, Laser spectroscopy for monitoring of radiocarbon in atmospheric samples, Anal. Chem. 91 (19) (2019) 12315–12320.
[15] A.J. Fleisher, D.A. Long, Q. Liu, L. Gameson, J.T. Hodges, Optical measurement of radiocarbon below unity fraction modern by linear absorption spectroscopy, J. Phys. Chem. Lett. 8 (2017) 4550–4556.
[16] M.G. Delli Santi, G. Insero, S. Bartalini, P. Cancio, F. Carcione, I. Galli, G. Giusfredi, D. Mazzotti, A. Bulgheroni, A.I. Martinez Ferri, et al., Precise radiocarbon determination in radioactive waste by a laser-based spectroscopic technique, Proc. Nat. Acad. Sci. 119 (28) (2022) e2122122119.
[17] J. Lehmuskoski, H. Vasama, J. Hämäläinen, J. Hokkinen, T. Kärkelä, K. Heiskanen, M. Reinikainen, S. Rautio, M. Hirvelä, G. Genoud, On-line monitoring of radiocarbon emissions in a nuclear facility with cavity ring-down spectroscopy, Anal. Chem. 93 (48) (2021) 16096–16104.
[18] K. Jiao, J. Gao, J. Yang, G. Zhao, Z. Shi, X. Wang, D. Zhu, H. He, J. Qing, X. Yan, et al., Spectroscopic detection of radiocarbon dioxide based on optical feedback linear cavity enhanced absorption spectroscopy, Microw. Opt. Technol. Lett. 66 (1) (2024) e33946.
[19] I. Galli, S. Bartalini, S. Borri, P. Cancio, D. Mazzotti, P. De Natale, G. Giusfredi, Molecular gas sensing below parts per trillion: Radiocarbon-dioxide optical detection, Phys. Rev. Lett. 107 (2011) 270802.
[20] I. Galli, S. Bartalini, R. Ballerini, M. Barucci, P. Cancio, M. De Pas, G. Giusfredi, D. Mazzotti, N. Akikusa, P. De Natale, Spectroscopic detection of radiocarbon dioxide at parts-per-quadrillion sensitivity, Optica 3 (4) (2016) 385–388.
[21] Y.-D. Tan, C.-F. Cheng, D. Sheng, S.-M. Hu, Detection of radiocarbon dioxide with double-resonance absorption spectroscopy, Chin. J. Chem. Phys. 34 (4) (2021) 373–380.
[22] A.D. McCartt, J. Jiang, Room-temperature optical detection of $^{14}CO_2$ below the natural abundance with two-color cavity ring-down spectroscopy, ACS Sens. 7 (2022) 3258–3264.
[23] J. Jiang, A.D. McCartt, Mid-infrared trace detection with parts-per-quadrillion quantitation accuracy: Expanding frontiers of radiocarbon sensing, Proc. Nat. Acad. Sci. 121 (15) (2024) e2314441121.
[24] K.K. Lehmann, Resonance enhanced two-photon cavity ring-down spectroscopy of vibrational overtone bands: A proposal, J. Chem. Phys. 151 (2019) 144201.
[25] K.K. Lehmann, Theoretical detection limit of saturated absorption cavity ring-down spectroscopy (scar) and two-photon absorption cavity ring-down spectroscopy, Appl. Phys. B 116 (2014) 147–155.
[26] Y.-Z. Liu, M.-Y. Yu, Y.-D. Tan, J. Wang, C.-F. Cheng, W. Jiang, S.-M. Hu, Midinfrared cavity-enhanced two-photon absorption spectroscopy for selective detection of trace gases, Anal. Chem. 97 (1) (2025) 848–853.
[27] Y.-Z. Liu, W.-T. Cai, Y.-D. Tan, T.-P. Hua, C.-F. Cheng, S.-M. Hu, Trace molecular detection with wavelength-modulated cavity-enhanced two-photon absorption spectroscopy, Appl. Phys. B 131 (5) (2025) 1–7.
[28] Z.-T. Zhang, Y. Tan, J. Wang, C.-F. Cheng, Y.R. Sun, A.-W. Liu, S.-M. Hu, Seeded optical parametric oscillator light source for precision spectroscopy, Opt. Lett. 45 (2020) 1013–1016.
[29] Z.-T. Zhang, C.-F. Cheng, Y.R. Sun, A.-W. Liu, S.-M. Hu, Cavity ring-down spectroscopy based on a comb-locked optical parametric oscillator source, Opt. Express 28 (2020) 27600–27607.
[30] L.-S. Ma, J. Ye, P. Dubé, J.L. Hall, Ultrasensitive frequency-modulation spectroscopy enhanced by a high-finesse optical cavity: theory and application to overtone transitions of C_2H_2 and C_2HD, J. Opt. Soc. Am. B 16 (12) (1999) 2255–2268.
[31] J. Wang, Y.R. Sun, L.-G. Tao, A.-W. Liu, S.-M. Hu, Communication: Molecular near-infrared transitions determined with sub-khz accuracy, J. Chem. Phys. 147 (9) (2017) 091103.
[32] Y.-D. Tan, C.-F. Cheng, Y. Tan, S.-M. Hu, Mid-infrared–near-infrared double-resonance spectroscopy of molecules with kilohertz accuracy, Opt. Lett. 49 (5) (2024) 1109–1112.
[33] G.-W. Truong, L.W. Perner, D.M. Bailey, G. Winkler, S.B. Cataño-Lopez, V.J. Wittwer, T. Südmeyer, C. Nguyen, D. Follman, A.J. Fleisher, et al., Mid-infrared supermirrors with finesse exceeding 400 000, Nat. Commun. 14 (2023) 7846.
[34] G. Winkler, L.W. Perner, G.-W. Truong, G. Zhao, D. Bachmann, A.S. Mayer, J. Fellinger, D. Follman, P. Heu, C. Deutsch, et al., Mid-infrared interference coatings with excess optical loss below 10 ppm, Optica 8 (5) (2021) 686–696.
[35] I. Galli, P.C. Pastor, G. Di Lonardo, L. Fusina, G. Giusfredi, D. Mazzotti, F. Tamassia, P. De Natale, The ν_3 band of $^{14}C^{16}O_2$ molecule measured by optical-frequency-comb-assisted cavity ring-down spectroscopy, Mol. Phys. 109 (17–18) (2011) 2267–2272.
[36] E.J. Zak, J. Tennyson, O.L. Polyansky, L. Lodi, N.F. Zobov, S.A. Tashkun, V.I. Perevalov, Room temperature line lists for CO_2 symmetric isotopologues with ab initio computed intensities, J. Quant. Spectrosc. Radiat. Transfer 189 (2017) 267–280.
[37] X. Huang, D.W. Schwenke, R.S. Freedman, T.J. Lee, Ames-2016 line lists for 13 isotopologues of CO_2: updates, consistency, and remaining issues, J. Quant. Spectrosc. Radiat. Transf. 203 (2017) (2016) 224–241.
[38] K.K. Lehmann, Two-photon absorption line shapes in the transit-time limit, J. Chem. Phys. 154 (2021) 104105.
[39] K.K. Lehmann, Optical cavity with intracavity two-photon absorption, J. Opt. Soc. Am. B 37 (2020) 3055–3062.
[40] W. Demtröder, Laser Spectroscopy: 1 Basic Principles, Springer, 2008.
[41] Q.-H. Liu, H. Zhang, L. Wen, Y. Xie, T. Yang, C.-F. Cheng, S.-M. Hu, X. Yang, Preparation of high vibrational states in the entire molecular beam, J. Phys. Chem. Lett. 15 (2024) 9926–9931.

Yandong Tan received the bachelor's degree from China University of Mining and Technology. He received his Ph.D. from the University of Science and Technology of

China (USTC) in 2024 and is currently a postdoctoral fellow there. His research interests include: isotope detection and precision molecular spectroscopy.

Yuzhong Liu received the bachelor's degree from North China Electric Power University. He is currently a Ph.D. student at the University of Science and Technology of China (USTC). His research interests include mid-infrared light sources and precision molecular spectroscopy.

Mengyi Yu received the bachelor's degree from Sichuan University. She is currently a Ph.D. student at the University of Science and Technology of China (USTC). Her research interests include precision molecular spectroscopy.

Zenan Wang received the bachelor's degree from North China Electric Power University. He is currently a Ph.D. student at the University of Science and Technology of China (USTC). His research interests include molecular spectroscopy.

Cunfeng Cheng is currently a professor at the University of Science and Technology of China (USTC). He received his B.S. degree from USTC in 2006 and his Ph.D. degree from the same university in 2012. His main research fields include selective excitation and detection of molecular single quantum states, trace molecular isotope detection, and precision molecular spectroscopy.

Shuiming Hu is currently a Chair Professor at the University of Science and Technology of China (USTC) and also affiliated with the Hefei National Laboratory for Physical Sciences at the Microscale. He obtained his B.S. degree in 1995 and Ph.D. degree in 2000 from USTC. His research focuses on precision spectroscopy of atoms and molecules, as well as quantum metrology. His research work has achieved the highest-precision measurement of transition frequencies in two-electron systems (including helium atoms and hydrogen molecules), and these results have been applied to the testing of fundamental physics, the determination of fundamental physical constants, and the measurement of nuclear parameters. In addition, the precision spectroscopy technologies and instruments he has developed have been used in high-precision metrology of gas content, temperature, and isotope concentration, promoting the transformation from traditional metrology to quantum metrology.